

# Grids of stellar models

## VII. From 0.8 to 60 $M_{\odot}$ at $Z = 0.10^*$

N. Mowlavi<sup>1</sup>, D. Schaerer<sup>2</sup>, G. Meynet<sup>1</sup>, P.A. Bernasconi<sup>1</sup>, C. Charbonnel<sup>3</sup>, and A. Maeder<sup>1</sup>

<sup>1</sup> Geneva Observatory, CH-1290 Sauverny, Switzerland

<sup>2</sup> Space Telescope Science Institute, 3700 San Martin Drive, Baltimore, MD 21218, U.S.A.

<sup>3</sup> Laboratoire d'Astrophysique de Toulouse, CNRS - UMR 5572, 14 Av. E. Belin, 31400 Toulouse, France

Received February 6; accepted July 22, 1997

**Abstract.** We present a new grid of stellar models from 0.8 to 60  $M_{\odot}$  at  $Z = 0.10$ , with mass loss and moderate overshooting, from the zero age main sequence to either the helium flash (low mass stars), the early AGB phase (intermediate-mass stars) or the end of carbon burning (massive stars). The calculations are done with opacities provided by Iglesias & Rogers (1993), completed by those of Alexander & Ferguson (1994) at low temperatures. This grid is a homogeneous extension to very high metallicity of the previous grids published by the Geneva group. It is useful for the study of galactic bulges, elliptical galaxies and eventually quasars. Calculations of stars more massive than 60  $M_{\odot}$  are not presented as these objects lose almost their entire mass during their main sequence phase, and are likely to end their life as white dwarfs.

**Key words:** stars: evolution — stars: Hertzsprung-Russell diagram — stars: interiors

evolved regions such as galactic bulges, elliptical galaxies and eventually quasars. In those environments, the metallicity might reach up to 3 to 5 times the solar one (see e.g. McWilliam & Rich 1994; see also Simpson et al. 1995). Metallicities up to 10 times have even been claimed in the case of quasars (Korista et al. 1996), but such values are highly uncertain. Papers IV and V have already presented the evolution of metal-rich stars at  $Z = 0.04$ , about twice the solar metallicity. In this paper, we present stellar models computed at  $Z = 0.1$ , i.e. at five times the solar metallicity.

Similar calculations have been published by Fagotto et al. (1994). Their calculations are, however, restricted to stellar masses  $M \lesssim 9 M_{\odot}$  and do not take into account mass loss during the evolution. Moreover, they used the old radiative opacities by Huebner et al. (1977).

The model ingredients are described in Sect. 2. Section 3 presents briefly the results. Directives on how to obtain the full data tables are given in Sect. 4.

A detailed analysis of the characteristics of metal-rich stars is presented in a parallel paper (Mowlavi et al. 1997).

### 1. Introduction

This new grid of stellar models is an extension of the previous ones computed by the Geneva Group (Schaller et al. 1992, hereafter Paper I; Schaerer et al. 1993a, Paper II; Charbonnel et al. 1993, Paper III; Schaerer et al. 1993b, Paper IV; Meynet et al. 1994, Paper V; Charbonnel et al. 1996, Paper VI; Bernasconi 1996; Charbonnel et al. 1997), presenting the evolution of stars from 0.8 to 60  $M_{\odot}$  for a metallicity of  $Z = 0.10$ .

A grid of stellar models at such high metallicity is well adapted for the study of stellar populations in highly

### 2. Input physics

The calculations are performed with the Geneva stellar evolutionary code, whose physical ingredients have been extensively described in the previous papers (see for example Papers I and IV). In accordance with those previous calculations, we apply a moderate overshooting for  $M \geq 1.25 M_{\odot}$  of  $d/H_p = 0.20$  at the border of the convective core as defined by the Schwarzschild criterion, where  $d$  is the overshooting distance and  $H_p$  the local pressure scale height.

The following improvements/modifications have been performed with respect to the previous grids in order to match the requirements for  $Z = 0.1$ :

*Send offprint requests to:* N. Mowlavi

\* Data available at the CDS via anonymous ftp 130.79.128.5 or via <http://cdsweb.u-strasbg.fr/Abstract.html>

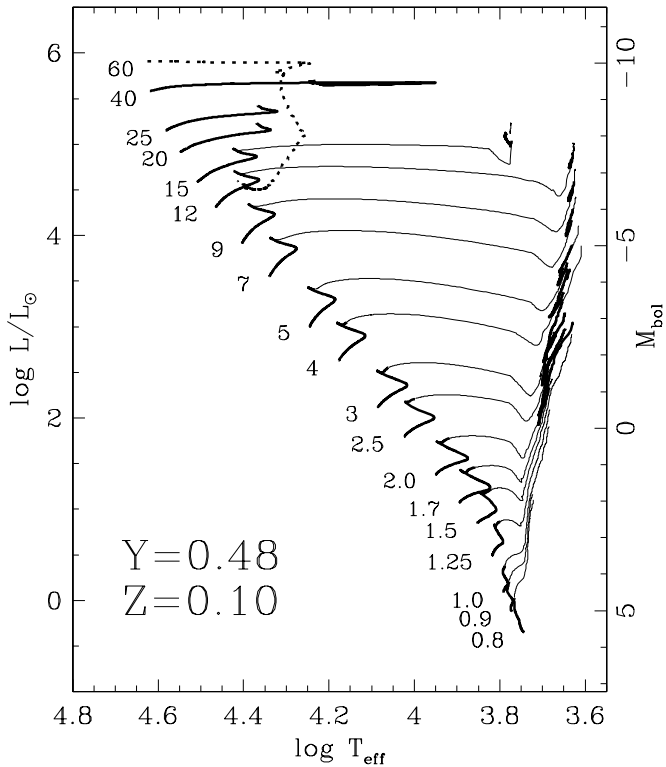


**Fig. 1.** Evolutionary tracks in the HR diagram for the models at  $Z = 0.1, Y = 0.48$  with mass loss and moderate overshooting. For clarity, only the main sequence has been drawn for  $M \geq 20 M_{\odot}$ , the full tracks of which are represented in Fig. 2. Thick parts of the tracks correspond to core H or He burning phases

- The initial helium content is taken as  $Y = 0.48$ . This follows from a cosmological helium abundance of  $Y|_{Z=0} = 0.24$  (Audouze 1987) and a relative conservative value of the ratio of helium to metal enrichment equal to  $\Delta Y/\Delta Z = 2.4$ . Other elemental abundances are taken from the solar distribution scaled to the metallicity.

- The radiative opacities for the interior are taken from Iglesias & Rogers (1996), while the low-temperature opacities are taken from Alexander & Ferguson (1994). The latter account for a wide variety of atomic and molecular species.

- At  $Z = 0.10$ , the criterion defining a star to be of the Wolf-Rayet type could be different from that at lower metallicities. However, in the absence of any observational counterpart of those objects at such high metallicities, we keep the same criterion as in Paper I, i.e. we consider that a star enters the WR stage when its surface hydrogen mass fraction becomes lower than 0.4 and its effective temperature is higher than 10000 K. The mass loss rates of these objects are then accordingly taken as in Paper I.

- The prescription for the mass loss rates at these high metallicities is quite uncertain. For consistency with

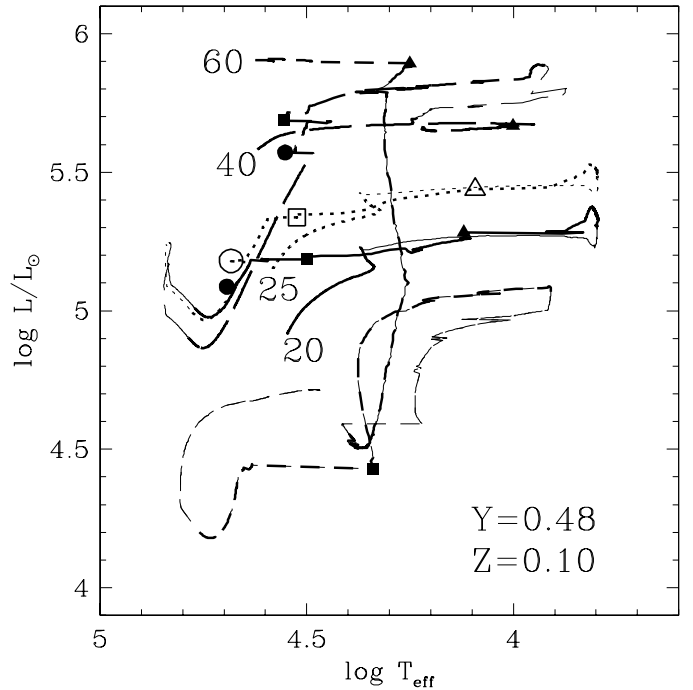


**Fig. 2.** Same as Fig. 1, but for the 20, 25 and  $40 M_{\odot}$  stars. Triangles, squares and circles locate the position of the stars on each track when they become WNL, WNE and WC, respectively. Open symbols refer to the  $25 M_{\odot}$  model star

**Table 1.** Core nuclear burning lifetimes at  $Z = 0.1, Y = 0.48$  (in  $10^n$  yr,  $n$  being given in parenthesis)

Initial mass	H-burning phase ( $t_H$ )	He-burning phase ( $t_{He}$ )	C-burning phase ( $t_C$ )	$t_{He}/t_H$
$60 M_{\odot}$	2.31(6)	1.19(6)	6.12(4)	0.515
40	2.17(6)	0.52(6)	1.62(4)	0.240
25	2.94(6)	0.54(6)	1.35(4)	0.184
20	3.57(6)	0.64(6)	1.33(4)	0.179
15	4.84(6)	0.79(6)	1.67(4)	0.163
12	6.44(6)	1.03(6)	2.79(4)	0.160
9	1.01(7)	1.67(6)	6.18(4)	0.165
7	1.63(7)	2.82(6)		0.173
5	3.58(7)	6.75(6)		0.189
4	6.43(7)	1.20(7)		0.187
3	1.47(8)	2.84(7)		0.193
2.5	2.53(8)	4.90(7)		0.194
2	4.97(8)	9.49(7)		0.191
1.7	8.23(8)	1.24(8)		0.151
1.5	1.22(9)			
1.25	2.17(9)			
1	3.84(9)			
0.9	5.69(9)			
0.8	8.84(9)			

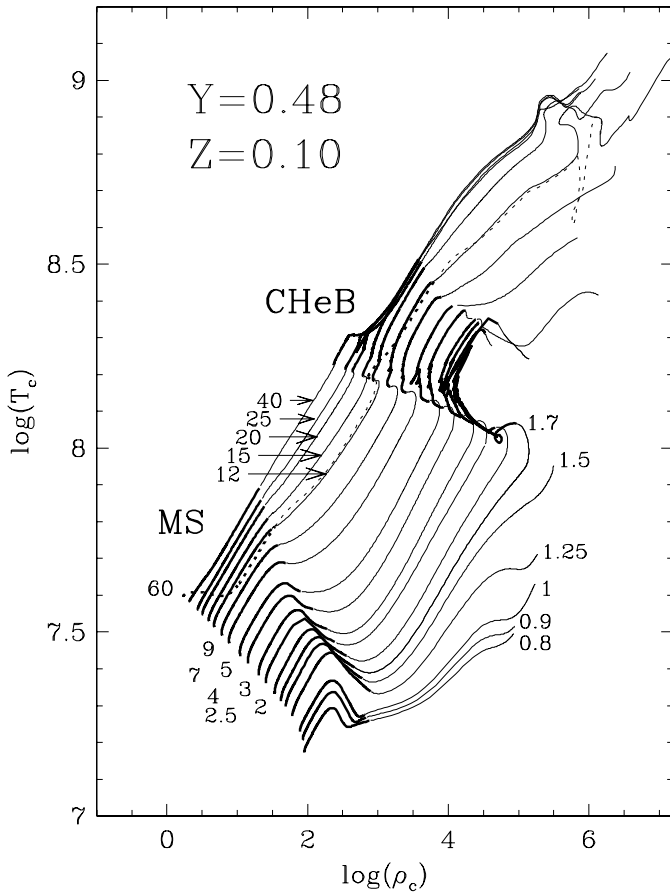


**Fig. 3.** Evolutionary tracks in the  $(\log \rho_c, \log T_c)$  diagram, where  $\rho_c$  and  $T_c$  are the central density and temperature, respectively, for the models at  $Z = 0.1, Y = 0.48$  with mass loss and moderate overshooting. Thick parts of the tracks correspond to the main sequence (MS) and core He burning (CHeB) phases. The labels on each track indicate the stellar initial masses

previous calculations performed at lower  $Z$ , we keep the same prescription as in Paper I, with, for all the non WR phases, a  $\dot{M}$  metallicity dependence as indicated by stellar wind models<sup>1</sup> (cf. Kudritzki et al. 1989), according to which  $(\dot{M}_Z/\dot{M}_{Z_\odot}) = (Z/Z_\odot)^{0.5}$ . Given the large main sequence (MS) mass loss and especially the low initial hydrogen content, very massive stars enter the WR phase rapidly during core hydrogen burning. Following the WR mass loss prescription, this leads to the ejection of almost the totality of the initial mass during the MS for  $M > 60 M_\odot$ . These stars would probably end as white dwarfs.

<sup>1</sup> Arguments have been presented in Paper V for the use of enhanced mass loss rates by a factor of two over the “standard” ones used in our other papers in this series. Such an enhancement has not been used in the present calculations. We expect that the mass loss rates driven by radiation pressure probably saturates at such a high metallicity. (Results of calculations at  $Z = 0.10$  and with enhanced mass loss rates are presented in IAU Symp. 184).

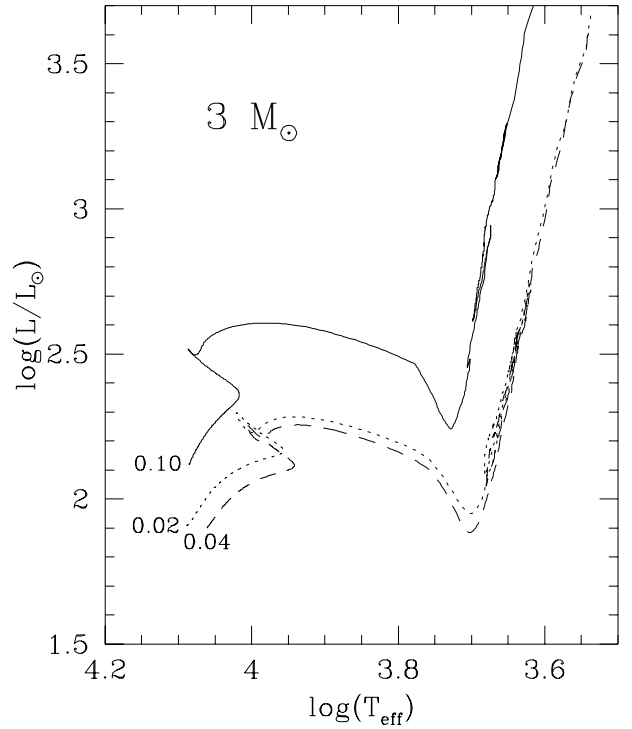


**Fig. 4.** Evolutionary tracks in the HR diagram for  $3 M_\odot$  star models at different metallicities as labeled on each track

Because of our total ignorance of the dependence of the mass loss rate on stellar characteristics in such conditions, we do not present evolutionary tracks for these stars.

### 3. Results

The evolution of 19 stars from  $0.8$  to  $60 M_\odot$  is followed from the zero age main sequence (ZAMS) up to either the He-flash for low-mass stars ( $M \leq 1.5 M_\odot$ ), to the early asymptotic giant branch (E-AGB,  $1.5 M_\odot < M \leq 9 M_\odot$ ), or to the end of core C-burning for massive stars ( $M > 9 M_\odot$ ).

The tracks in the Hertzsprung-Russell (HR) and in the  $\log T_c$  versus  $\log \rho_c$  diagrams are given in Figs. 1 to 3, while the lifetimes (as defined in Paper I) in the different nuclear burning phases and the ratio  $t_{\text{He}}/t_{\text{H}}$  of the lifetimes in the He- and H-burning phases are summarized in Table 1.

Interesting properties of the high metallicity models emerge when compared to lower metallicity ones. A detailed analysis is presented in a separate paper (Mowlavi et al. 1997). Let us just mention here that:

- the tracks at  $Z = 0.10$  are hotter and more luminous than the ones at  $Z = 0.04$  or  $0.02$  presented in Papers II and III. This is illustrated in Fig. 4 for a  $3 M_\odot$  track;
- as a consequence of the lower initial hydrogen content and higher luminosities, both the MS and the core helium burning (CHeB) phases are much shorter than the corresponding lifetimes of the previous calculations at  $Z \leq 0.04$  (a factor 2 to 3 as compared to the  $Z = 0.04$  models);

- hydrogen burns in a convective core during the MS in all our models down to  $0.8 M_{\odot}$ ;
- the maximum initial mass leading to the helium flash at the onset of CHeB is  $1.5 M_{\odot}$ .
- the  $60 M_{\odot}$  star enters the WNL phase very early during core hydrogen burning, and loses  $\sim 5 M_{\odot}$  during the MS. This rapid decrease in the total mass translates to a drop in the surface luminosity by  $\sim 1.5$  orders of magnitudes. The subsequent phase of rapid, as compared to mass-loss time-scale, core contraction enables the star to enter the CHeB phase without further appreciable mass loss, and the star evolves towards a WNE Wolf-Rayet star. As for stars more massive than  $60 M_{\odot}$ , the adopted mass loss prescription leads to the ejection of their entire mass during the MS. They never reach the He-burning phase, and are likely to end their life as helium white dwarfs.

**Table 2.** Times spent by the massive models with  $Z = 0.1, Y = 0.48$  as WNL, WNE and WC Wolf-Rayet stars (in  $10^6$  yr)

Initial mass	WNL	WNE	WC
$60 M_{\odot}$	1.392	1.216	–
40	0.169	0.041	0.440
25	0.017	0.144	0.203
20	0.015	0.134	0.135

- the lower initial mass leading to WR stars is  $\sim 17 M_{\odot}$ . Both the 20 and  $25 M_{\odot}$  models reach successively the WNL, WNE and WC Wolf-Rayet stages during their CHeB phases. The  $40 M_{\odot}$  model becomes a WNL during its MS, and WNE and WC during its CHeB phase. The  $60 M_{\odot}$  model also becomes a WNL during its MS and a WNE during its CHeB phase, but does not become a WC star, at least before the end of its core C burning phase. The times spent by the models as WNL, WNE or WC Wolf-Rayet stars are summarized in Table 2.

#### 4. How to obtain the tables electronically

The following data is available for each model:

$\log L/L_{\odot}$ ,  $\log T_{\text{eff}}$ ,  $X_{\text{s}}(\text{H})$ ,  $X_{\text{s}}(^4\text{He})$ ,  $X_{\text{s}}(^{12}\text{C})$ ,  $X_{\text{s}}(^{13}\text{C})$ ,  $X_{\text{s}}(^{14}\text{N})$ ,  $X_{\text{s}}(^{16}\text{O})$ ,  $X_{\text{s}}(^{17}\text{O})$ ,  $X_{\text{s}}(^{18}\text{O})$ ,  $X_{\text{s}}(^{20}\text{Ne})$ ,  $X_{\text{s}}(^{22}\text{Ne})$ ,  $Q_{\text{cc}}$ ,  $T_{\text{eff,uncor}}$ ,  $\log(-\dot{M})$ ,  $\log \rho_{\text{c}}$ ,  $\log T_{\text{c}}$ ,  $X_{\text{c}}(\text{H})$ ,  $X_{\text{c}}(^4\text{He})$ ,  $X_{\text{c}}(^{12}\text{C})$ ,  $X_{\text{c}}(^{13}\text{C})$ ,  $X_{\text{c}}(^{14}\text{N})$ ,  $X_{\text{c}}(^{16}\text{O})$ ,  $X_{\text{c}}(^{17}\text{O})$ ,  $X_{\text{c}}(^{18}\text{O})$ ,  $X_{\text{c}}(^{20}\text{Ne})$ ,  $X_{\text{c}}(^{22}\text{Ne})$

where  $X_{\text{s}}$  and  $X_{\text{c}}$  are the abundances, in mass fractions, at the surface and at the center of the star, respectively,  $Q_{\text{cc}}$  the convective core mass fraction (overshooting included),  $T_{\text{eff,uncor}}$  the uncorrected value of  $T_{\text{eff}}$  (for WR stars only),

and  $\rho_{\text{c}}$  and  $T_{\text{c}}$  the central density and temperature, respectively. More detailed descriptions of the model selection and the table contents are given in Paper I.

These data, as well as the ones relative to the previous published grids (Papers I to VI), are accessible electronically at the Centre de Données Stellaires de Strasbourg (CDS, see A&A 1992, Vol. 266 No. 2, page E1, or at <http://cdsweb.u-strasbg.fr/CDS.html>). The data can also be obtained from the Geneva Observatory by means of anonymous ftp at [obsftp.unige.ch](ftp://obsftp.unige.ch) in the directory *pub/evol/modelz100*, or through the Web at <http://obswww.unige.ch>.

*Acknowledgements.* We thank Drs. D.R. Alexander and J.W. Ferguson for providing us with the low temperature opacity tables.

#### References

- Alexander D.R., Ferguson J.W., 1994, ApJ 437, 879  
 Audouze J., 1987, Observational Cosmology, IAU Symp. 124, Hewitt A. et al. (eds.). Reidel, p. 89  
 Bernasconi P.A., 1996, A&AS 120, 57  
 Charbonnel C., Meynet G., Maeder A., Schaerer D., 1996, A&AS 115, 339 (Paper VI)  
 Charbonnel C., Meynet G., Maeder A., Schaller G., Schaerer D., 1993, A&AS 101, 415 (Paper III)  
 Charbonnel C., Wäppen W., Bernasconi P., et al., 1997, A&AS (in preparation)  
 Fagotto F., Bressan A., Bertelli G., Chiosi C., 1994, A&AS 105, 39  
 Huebner W.F., Mertz A.L., Magee N.H., Argo M.F., 1977, Los Alamos Scientific Laboratory Report LA-6760-M  
 Iglesias C.A., Rogers F.J., 1996, ApJ 464, 943  
 Korista K., Hamann F., Ferguson J., Ferland G., 1996, ApJ 461, 641  
 Kudritzki R.P., Pauldrach A., Puls J., Abbott D.C., 1989, A&A 219, 205  
 Meynet G., Maeder A., Schaller G., Schaerer D., Charbonnel C., 1994, A&AS 103, 97 (Paper V)  
 Mowlavi N., Meynet G., Maeder A., Schaerer D., Bernasconi P.A., Charbonnel C., A&A (in preparation)  
 Schaerer D., Charbonnel C., Meynet G., Maeder A., Schaller G., 1993b, A&AS 102, 339 (Paper IV)  
 Schaerer D., Meynet G., Maeder A., Schaller G., 1993a, A&AS 98, 523 (Paper II)  
 Schaller G., Schaerer D., Meynet G., Maeder A., 1992, A&AS 96, 269 (Paper I)  
 Simpson J.P., Colgan S.W., Rubin R.H., Erickson E.F., Haas M.R., 1995, ApJ 444, 721  
 McWilliam A., Rich R.M., 1994, ApJS 91, 749